Mobile Radiosonde Deployments During the Mesoscale Predictability Experiment (MPEX)

Rapid and Adaptive Sampling of Upscale Convective Feedbacks

BY ROBERT J. TRAPP, DAVID J. STENSRUD, MICHAEL C. CONIGLIO, RUSS S. SCHUMACHER, MICHAEL E. BALDWIN, SEAN WAUGH, AND DON T. CONLEE

The Mesoscale Predictability Experiment (MPEX) was a field campaign conducted 15 May through 15 June 2013 within the Great Plains region of the United States. MPEX had two complementary research foci:

- *Focus 1:* The effects of upstream, prestorm mesoscale and subsynoptic-scale environmental features on regional-scale numerical weather prediction (NWP) of convective storms.

- *Focus 2:* The upscaling effects of isolated deep-convective storms on their environment, and the feedback of these effects to the convective-scale dynamics and predictability.

An overview of these foci and the multiple facets of the MPEX operations can be found in Weisman et al. (2015). The purpose of this brief but complementary article is to highlight Focus 2 activities. In particular, we describe both the feasibility and limitations of launching balloon-borne GPS radiosondes from ground-based mobile platforms, in ways meant to mimic airborne dropsonde deployments. Documentation of our experiences is provided here for the benefit of future field experiments that need, as we did, an alternative to dropsondes over land and in the vicinity of active convection.

AFFILIATIONS: TRAPP—University of Illinois at Urbana-Champaign, Urbana, Illinois; STENSRUD—The Pennsylvania State University, University Park, Pennsylvania; CONIGLIO AND WAUGH—NOAA/National Severe Storms Laboratory, Norman, Oklahoma; SCHUMACHER—Colorado State University, Ft. Collins, Colorado; BALDWIN—Purdue University, West Lafayette, Indiana; CONLEE—Texas A&M University, College Station, Texas

CORRESPONDING AUTHOR: Robert J. Trapp, Department of Atmospheric Sciences, University of Illinois at Urbana-Champaign, 105 S. Gregory Street, Urbana, IL 61801

E-mail: jtrapp@illinois.edu

DOI:10.1175/BAMS-D-14-00258.1

A BRIEF BACKGROUND. Within unstable, unsaturated layers, vertical circulations associated with the resultant convection mix high (low) virtual potential temperature air upward (downward), and thereby adjust the lapse rate of the convecting layer of air back toward a more statically stable state. Indeed, this idea of convective adjustment forms the basis for convective parameterization schemes in NWP models. But other processes besides vertical mixing are also at play in deep cumulus convection. For example, deep convective clouds diabatically heat the atmosphere when water vapor condenses into cloud droplets, and diabatically cool the atmosphere when subsequent precipitation falls out of the cloud and evaporates. Such diabatic heating, especially when sustained through mesoscale convective systems (MCSs), can lead to long-lasting modifications of the larger-scale geopotential height and wind field in the middle- and upper-troposphere. Diabatic cooling associated with precipitating downdrafts can result in a pool of cool air at the ground that spreads laterally away from the precipitating cloud. Both are forms of upscale feedbacks that have local as well as remote effects on the atmosphere and its ability to support subsequent cumulus convection. And, as supported by previous work, these effects are realized as measurable perturbations to the vertical distributions of atmospheric temperature, humidity, and wind.

Misrepresentation of, for example, the depth or areal extent of a surface cold pool in NWP models will

necessarily induce some error in subsequent predictions of temperature, cloud coverage, precipitation, etc., at and beyond the scales commensurate with the several-kilometer grid lengths now used in high-resolution convection-permitting models. It is unclear, however, how the magnitudes of this and the other feedbacks, and the ultimate larger-scale and longer-term consequence of their misrepresentation, vary with the convective intensity and morphology. Consider that relative to ordinary convective storms, supercell thunderstorms possess large, intense, and long-lived updrafts and downdrafts owing to their unique dynamics. The implication is that an outbreak of supercell thunderstorms, and perhaps even an isolated supercell, should have comparatively large upscale feedbacks. Accordingly, supercells were specifically targeted during MPEX.

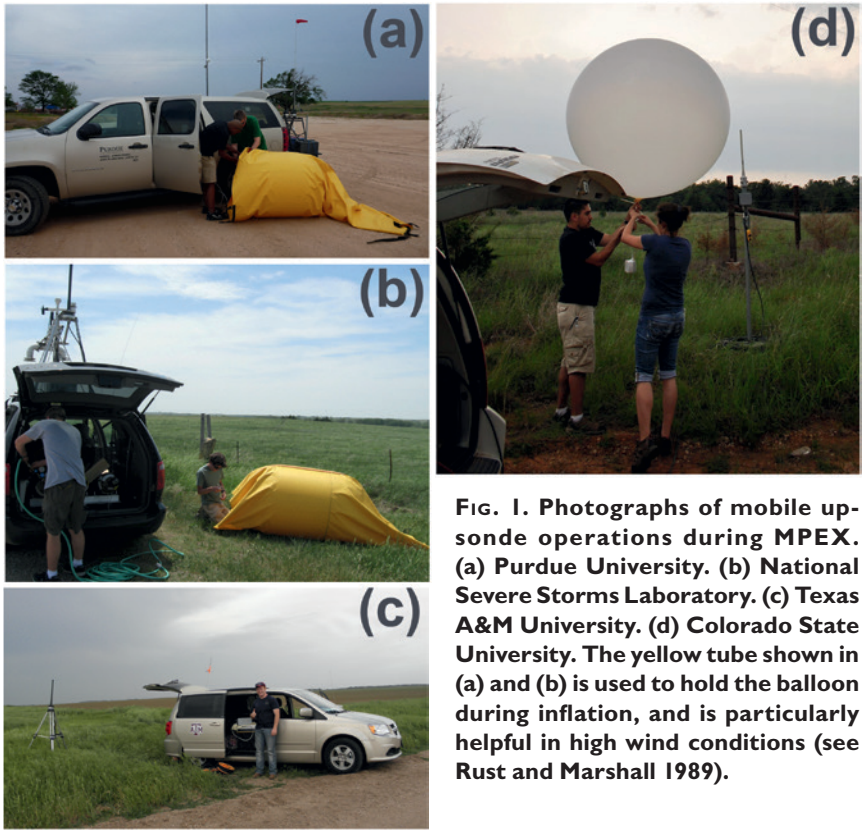

Fig. 1. Photographs of mobile upsonde operations during MPEX. (a) Purdue University. (b) National Severe Storms Laboratory. (c) Texas A&M University. (d) Colorado State University. The yellow tube shown in (a) and (b) is used to hold the balloon during inflation, and is particularly helpful in high wind conditions (see Rust and Marshall 1989).

Attempts to quantify and otherwise characterize the 3D atmosphere near supercells are not unique to MPEX. Large field campaigns [such as the Verification of the Origins of Rotation (VORTEX) and VORTEX2] and even smaller-scale projects have included efforts to collect radiosonde observations within supercells and in their environments. But in contrast to the upscale focus of MPEX, the prior field studies were focused primarily on quantifying the environmental characteristics that beget the convective storms, which essentially is a downscaling perspective. Thus, even though VORTEX2 upsonde operations were, for example, mobile and storm-following, they were designed to examine the variability of the mesoscale environment and how this may impact tornado formation (e.g., Parker 2014).

UPSONDE SYSTEMS. Teams from Purdue University (PU), the National Severe Storms Laboratory (NSSL), Colorado State University (CSU), and Texas A&M University (TAMU) fielded mobile radiosonde systems during MPEX (Fig. 1). As detailed in Table 1, PU, NSSL, and TAMU used systems manufactured by International Met Systems (iMet), and CSU employed a Vaisala system. The iMet sondes were preconfigured with four frequency options, and iMet provided MPEX investigators with a separate batch of sondes with four

Table 1. Details of radiosonde systems employed during MPEX.

Team	Model	Sonde types	Balloon
PU	iMet 3050 (2)	iMet-1-AB 403 MHz GPS radiosondes	200-g latex
NSSL	iMet 3050, and iMet 3150	iMet-1-AB 403 MHz GPS radiosondes	200-g latex
CSU	Vaisala Digicora MW21	Vaisala RS92 radiosondes	200-g latex
TAMU	iMet 3050 (and iMet 3150 for redundancy)	iMet-1-AB, and iMet-1-AA 403 MHz GPS radiosondes	200-g latex

additional frequencies. These eight frequency options combined with the narrow transmission band of the iMet sondes allowed the teams to conduct operations without being concerned with frequency overlap.

In fact, PU and NSSL both had the capability to simultaneously receive signals from two separate sondes that were transmitting at different frequencies. When combined with the single frequency systems of CSU and TAMU (whose participation was limited to 23–31 May 2013),[1] simultaneous sampling with six sondes was afforded. Moreover, because of vehicle-mounted antennas and a mobile power source (via an inverter) in the PU, NSSL, and TAMU systems, signal reception while mobile was fully enabled and generally without issue.

The use of 200-g balloons allowed the sondes to ascend well above the tropopause within 45 to 60 min after launch, after which time the data collection usually was terminated owing to a typically weak sonde signal or balloon burst. At this time, CSU and TAMU could launch a new sonde using a different frequency. PU and NSSL could, on the other hand, launch a new sonde at any time, and on occasion did so at approximately 15-min intervals; in practice, and given acceptable and safe launch conditions, PU and NSSL typically staggered their individual launches by 30 min, so that they each could keep two sondes in the air continuously. It is noteworthy to mention here that the time to configure the sonde, enter needed data into the receiving system, and inflate the balloon varied depending upon operator experience and weather conditions, but typically took only 5–10 min.

Laptop computers were used to process the radiosonde data in real time. These data were often used by the in-field Upsonde Director (UD) to make deployment decisions, especially during preconvective periods. Pre- and active-convection deployment decisions made by the UD were also facilitated by the in-field availability of real-time radar and other meteorological data. In fact, knowledge of team location relative to observed storm structure and other mesoscale features was paramount to the successful execution of the types of sampling strategies described in the sections that follow.

DATA QUALITY CONTROL AND SONDE INTERCOMPARISON. Although the iMet and Vaisala systems both offered data quality control (QC) during initial processing, additional QC was performed by the individual teams and by NCAR EOL personnel at the completion of the field campaign. For example, sonde data collected after balloon burst were manually removed, as were spurious data that were recorded following, say, an unintended sonde passage through a downdraft. Intercomparisons of soundings were used to check for any obvious inconsistencies in observed GPS altitude, pressure, and other variables.

To examine the viability of intermixing the two different sondes for environmental sampling, a comprehensive intercomparison between the iMet and Vaisala sondes was made prior to the field campaign. On 14 days during May 2012, an iMet-1 AB sonde and a Vaisala RS92 sonde were suspended from the same 200-g balloon and launched from the same location in Norman, Oklahoma, in the daytime (between 1400 UTC and 2000 UTC). The measurements made by the two sondes had very small differences in temperature, with the median difference less than 0.5 K everywhere below 200 hPa (Fig. 2a). The iMet sonde relative humidity was slightly lower in the boundary layer (median values ~ -2%) and slightly higher in the 500–300 hPa layer (median values ~ +2%) (Fig. 2a), but overall the differences were small everywhere in the troposphere.

ENVIRONMENTAL SAMPLING STRATEGIES. The two basic objectives of the upsonde teams were to sample the mesoscale environment over regions of anticipated convection initiation (CI), and then to sample the mesoscale environment that had been disturbed by subsequent convective storms. These objectives were accomplished through preconvective environment (PCE) strategies and convectively disturbed environment (CDE) strategies, respectively.

PCE Sampling. The full tropospheric structure of the mesoscale environment, prior to and in the region of anticipated CI, was sampled with a PCE strategy. During a typical PCE deployment, the upsonde teams were positioned relative to the time and location of expected CI, with the first upsonde observations made upstream of the expected CI location, and the last observations made downstream of and near the time of CI occurrence. This strategy allowed for data collection on the presumed contributor to CI (e.g., a mesoscale boundary), and then concluded with favorable positioning of the teams for CDE deployment. Most importantly, it allowed for samples of the preconvective environment (and its mesoscale

[1] TAMU periodically collected upsonde observations at College Station, Texas, at other times during the field campaign.

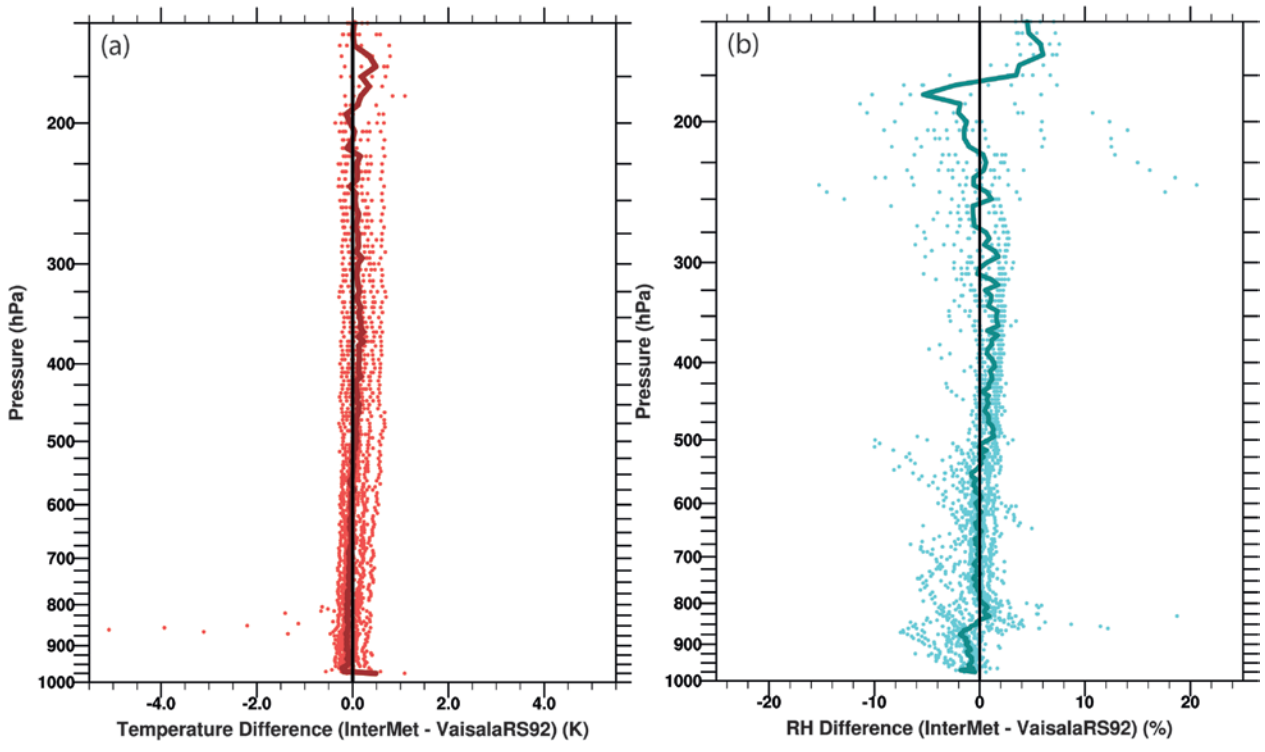

Fig. 2. Difference in (a) temperature (K) and (b) relative humidity (%) between InterMet and Vaisala RS92 sondes from 14 intercomparison flights. Dots are the differences for each flight and the solid line is the median difference.

variability) that could later be compared to samples of the convectively disturbed environment.

The range of PCE deployments during the project depended mostly on the expected CI mechanism and location, and surprisingly little on identification of suitable observation sites. Indeed, the teams quickly became adept at site identification and rapid deployment. Guided by an experimental ensemble of convection-permitting NWP models and by operational meteorological information, an initial target domain was typically identified by 1500 UTC, with data collection beginning between 1800 and 2000 UTC, but was delayed to as late as 2100 UTC. Given a choice of more than one domain, preference was often given to the one that showed more uncertainty in storm occurrence within the model ensemble, to accommodate later studies on the impact of the assimilation of the PCE soundings on model forecasts of the event.

The preconvective operations on 20 May 2013 exemplify the type of PCE sampling that was envisioned in the experimental plan. At ~1715 UTC, the PU, CSU, and NSSL teams sampled the preconvective environment west of a zone of enhanced mesoscale convergence in central Oklahoma, and east of a more extensive quasistationary boundary; these launches were also coordinated in time with the National Weather Service radiosonde launch at Norman, Oklahoma (Fig. 3). Thereafter, PU redeployed to the east-northeast of its initial position, to facilitate PCE sampling in the vicinity and east of the convergence zone at ~1815 UTC. Local CI occurred west of the array at approximately this same time, albeit in association with the quasistationary boundary rather than the more subtle convergence zone. By 2000 UTC, one of the convective cells had matured into a tornadic supercell near Marlow, Oklahoma, and within the next two hours would move through the region that had been sampled previously (and also sampled subsequently, using the CDE strategies).

Although analysis of the upsonde data from this case is ongoing, the PCE (and CDE) samples have already revealed interesting contrasts in boundary layer evolution that depend on storm-relative launch locations. For example, the CSU soundings at 1714 UTC (not shown), 1827 UTC, and 2030 UTC (Fig. 4a), which were collected in the preconvective environment and then inflow of the supercell, show a gradual *deepening* in the height of the capping inversion and thus increase in the convective boundary layer depth, presumably owing to large-scale ascent.

The PU soundings at 1815 UTC (Fig. 3b), 1958 UTC (not shown), and 2045 UTC (Fig. 4b), which were collected in the preconvective environment and then downwind of the supercell, show a gradual *lowering* of the inversion and boundary layer depth; note that the launch locations of CSU and PU prior to 2000 UTC were separated by only 22 km (Fig. 3). Accounting for the sonde drift during data collection (see Fig. 3), this contrasting evolution in the PU-sampled boundary layer could have resulted from low-level (~850 hPa) adiabatic descent and warming (and drying) in proximate subsidence, and from midlevel (~750 hPa) diabatic cooling in a weak unsaturated downdraft farther downwind underneath the anvil of the approaching supercell. Numerical model simulations of this and other cases are being used to help provide further insight into these possible upscale effects.

CDE Sampling. CDE strategies were used to sample the full tropospheric structure of the mesoscale environment in close proximity to intense convective storms. During typical CDE deployments, the upsonde teams executed time-coordinated sonde launches at 30-min intervals (60-min intervals for CSU and TAMU) at locations relative to the convective-storm motion

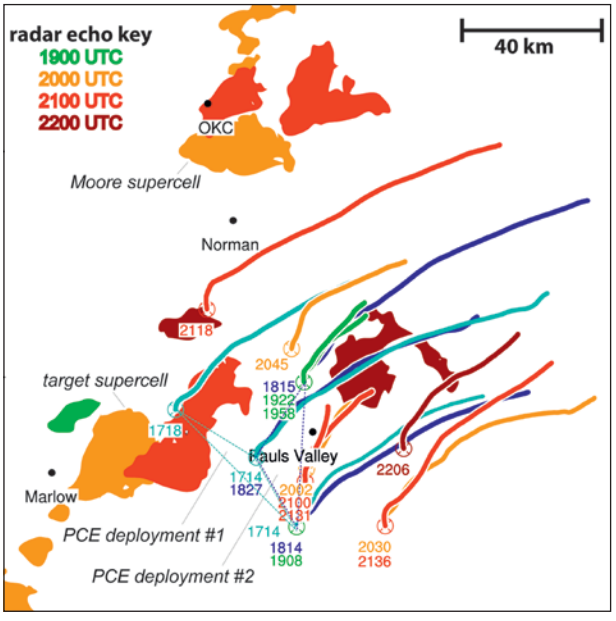

Fig. 3. PCE sampling on 20 May 2013. Hybrid-scan radar reflectivity factor ≥ 45 dBZ from the NSSL multiradar, multisensor analysis is shown by the filled contours, which are color coded by time (UTC) to match the color of the lines depicting the trajectory of the radiosonde flights within that hour. Thin dashed lines serve to highlight select coordinated radiosonde observations. To enhance clarity of the presentation, some radar echoes outside the immediate sampling area have been removed.

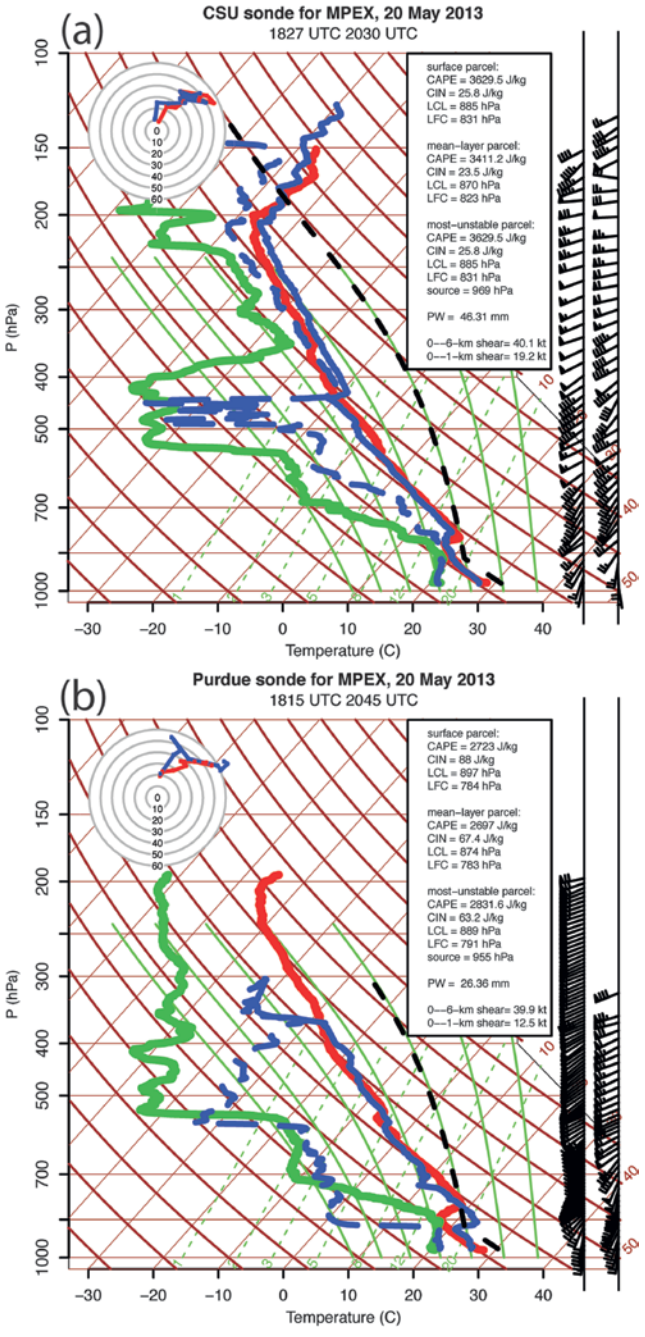

Fig. 4. Boundary layer evolution on 20 May 2013, as revealed through MPEX upsonde operations. (a) CSU soundings in a skew *T*–log*p* diagram at 1827 UTC (red/green) and 2030 UTC (blue/blue dashed). (b) PU soundings in a skew *T*–log*p* diagram at 1815 UTC (red/green) and 2045 UTC (blue/blue dashed). See Fig. 3 for sounding locations.

vector. Such storm-relative sampling was facilitated by the use of a combination of mobile communications (an MPEX chatroom, text messages, and cellular phone calls) and weather radar displays with real-time overlays of vehicle positions. The launch positions and launch times were determined by the UD and were based upon the evolving storm characteristics, our general operating plan, and the road network. Lapses in communication often forced the teams to operate autonomously, but nonetheless the teams were often still able to time-coordinate their respective launches in their designated storm-relative locations. The PU and NSSL teams would then immediately go mobile to get into position for the next launch.

The CDE operations on 19 May 2013 illustrate the adaptive and innovative strategies employed during MPEX. After the PCE sampling at 1900 UTC, the upsonde teams targeted a rapidly intensifying cell located upstream from their north-central Oklahoma locations. Accounting for the storm-motion vector, the teams redeployed east and south, such that NSSL and CSU (PU) would be north (south) of the cell that would ultimately spawn a tornado near Edmond, Oklahoma (Fig. 5). Environmental soundings were collected as the now tornadic supercell moved through this north-south array. Subsequently, the teams redeployed farther south and east to target the supercell that produced a tornado near Shawnee, Oklahoma. The environment disturbed by this supercell was nominally sampled at 0045 UTC using a triangular array that yielded a wake sounding, an inflow sounding, and a downstream sounding (Fig. 5). These soundings are shown in Weisman et al. (2015), who note that other than the (temperature, moisture, and wind) changes induced at low levels by the cold pool, the environmental structure in the immediate wake of the Shawnee supercell was relatively unmodified.

Note that in this case and others, an offset distance between the launch location and the edge of the convective echo was chosen to be ~10–20 km, but ultimately depended on suitable roads and the storm motion. Also in this case, east-west staggering was introduced to the launch locations when possible, to result in observation "triangles." These will facilitate the calculation of kinematic quantities (vorticity, divergence) using the triangle method.

Although operations preference was given to slow-moving supercellular convection (see Table 2), other modes of convection were also targeted. For example, consider the CDE operations on 29 May 2013. Upon completion of PCE soundings in the northwest

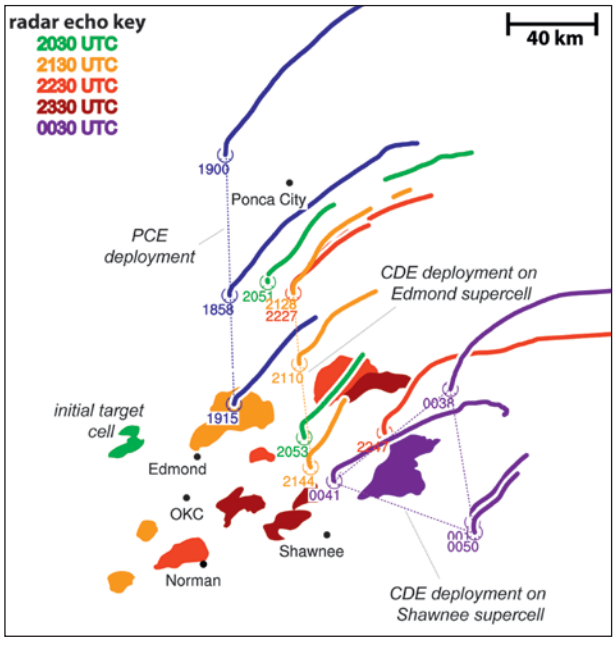

Fig. 5. As in Fig. 3, except on 19–20 May 2013.

Oklahoma/northeast Texas Panhandle at 1800 UTC, the four teams rotated their "box" pattern counterclockwise into a "diamond" pattern to better surround an approaching target cell that had developed well southwest of Canadian, Texas (Fig. 6). The expectation was that this cell would transition into a supercell by

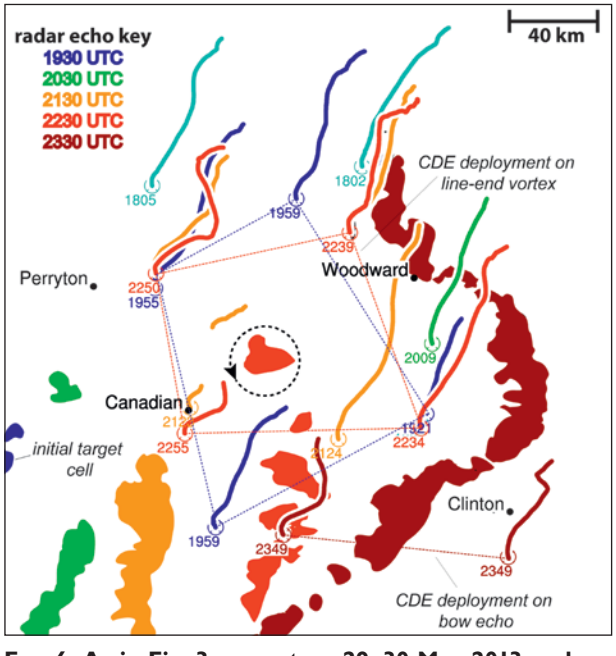

Fig. 6. As in Fig. 3, except on 29–30 May 2013 and reflectivity ≥ 40 dBZ.

the time it reached the upsonde array, so coordinated soundings were taken at ~2000 UTC. After 2000 UTC, however, the target cell began to dissipate, so a decision was made to consider the convective line that was developing southwest of the array. As the convective line evolved into a squall-line bow echo, the teams were able to reorient their array and at ~2240 UTC successfully sample the environment disturbed by the northern line-end vortex and associated deep convection (Fig. 6). A final set of soundings was collected at 2349 UTC by two teams, who were able to rapidly redeploy to the south and simultaneously sample the inflow and outflow of the squall-line bow echo.

CONCLUDING REMARKS. The improvements in the cost, reliability, and usability of radiosonde systems and mobile communications led to a unique application of these observing systems during MPEX. What was initially envisioned as an aircraft-only data collection experiment evolved into one that included mobile ground-based operations, wherein upsondes were launched at high rates in locations around moving convective storms throughout their life cycles. In fact, ground-based operations had the distinct advantage of being free from air-traffic control and other aircraft logistics, which thus allowed for relatively more flexibility in targets and strategy. Given the use of graduate and undergraduate students to assist in the field deployments, and an availability of relatively low-cost yet high-quality radiosonde systems, the cost of the ground-based operations was also comparatively lower. Of course, (storm-following)

TABLE 2. Summary of upsonde deployments during MPEX.

Date	Brief description
15 May	Northern Texas, tornadic supercell (NSSL-only deployment)
16 May	Southwestern Kansas, convective cells; coordination test
18 May	West-central Kansas tornadic supercell
19 May	Central Oklahoma, two tornadic supercells
20 May	Central Oklahoma, tornadic supercell
23 May	Northwestern Texas, tornadic supercell, with wake/cold pool soundings, and some inflow soundings into developing MCS
27 May	Central Kansas, intense cell with some supercell characteristics
28 May	South-central Kansas, demise of intense cell
29 May	Western Oklahoma/eastern Texas Panhandle, developing bow echo, with surround sampling of the northern bookend vortex, and additional sampling of cold pool and inflow of QLCS
30 May	South-central Oklahoma, nontornadic supercell (all teams), and some Purdue-only sampling of wake of additional nontornadic supercell
31 May	Central Oklahoma, tornadic supercell
3 June	Oklahoma Panhandle, southwest Kansas, intense cells with some (HP) supercell characteristics, surround strategy, then additional sampling of developing bow echo
4 June	Eastern Texas Panhandle, mesoscale environment
8 June	Southwest Kansas, Oklahoma Panhandle, intense cell within line
11 June	Western Nebraska, weak convection and additional cell
12 June	Eastern Wyoming, mesoscale environment
14 June	Kansas–Colorado, weak convective line

ground-based operations will always be limited by suitable road and deployment-site availability, and inherently by the storm movement relative to allowable driving speeds. Thus, one trade-off is a relatively reduced area of sounding coverage per time interval.

In future field campaigns, inclusion of additional upsonde teams would help ground-based upsonde operations approach parity with airborne dropsonde operations. This is most relevant when the logistics of the scientific problem and observational domain render airborne deployments infeasible. As one example, similar observation strategies with mobile upsondes were used to investigate nocturnal convective systems in the Plains Elevated Convection at Night (PECAN) experiment, held in 2015 within the Great Plains region of the United States.

FOR FURTHER READING

Bluestein, H. B., 1999: A history of severe-storm-intercept field programs. *Wea. Forecasting,* **14,** 558–577, doi:10.1175/1520-0434(1999)014<0558:AHOSSI>2.0.CO;2.

Bretherton, C. S., 1993: The nature of adjustment in cumulus cloud fields. *The Representation of Cumulus Convection in Numerical Models, Meteor. Monogr.*, No. 46, Amer. Meteor. Soc., 63–74.

Parker, M. D., 2014: Composite VORTEX2 supercell environments from near-storm soundings. *Mon. Wea. Rev.,* **142,** 508–529, doi:10.1175/MWR-D-13-00167.1.

Rust, W. D., and T. C. Marshall, 1989: Mobile, high-wind, balloon-launching apparatus. *J. Atmos. Oceanic Technol.,* **6,** 215–217, doi:10.1175/1520-0426(1989)006<0215:MHWBLA>2.0.CO;2.

——, D. W. Burgess, R. A. Maddox, L. C. Showell, T. C. Marshall, and D. K. Lauritsen, 1990: Testing a Mobile Version of a Cross-Chain Loran Atmospheric (M-CLASS) sounding system. *Bull. Amer. Meteor. Soc.,* **71,** 173–180, doi:10.1175/1520-0477(1990)071<0173:TAMVOA>2.0.CO;2.

Spencer, P. L., D. J. Stensrud, and J. M. Fritsch, 2003: A method for improved analyses of scalars and their derivatives. *Mon. Wea. Rev.,* **131,** 2555–2576, doi:10.1175/1520-0493(2003)131<2555:AMFIAO>2.0.CO;2.

Trapp, R. J., 2013: *Mesoscale-Convective Processes in the Atmosphere.* Cambridge University Press, 346 pp.

Weisman, M. L., and Coauthors, 2015: The Mesoscale Predictability Experiment (MPEX). *Bull. Amer. Meteor. Soc.,* **96**, 2127–2149, doi:10.1175/BAMS-D-13-00281.1.